Scarcity of fixed carbon transfer in a model microbial phototroph-heterotroph interaction

Short Title: Scarcity of microbial carbon transfer

Sunnyjoy Dupuis[1,2], Usha F. Lingappa[2], Xavier Mayali[3], Eve S. Sindermann[2], Jordan L. Chastain[2,4], Peter K. Weber[3], Rhona Stuart[3], Sabeeha S. Merchant[1,2,5,6]

[1]Department of Plant and Microbial Biology, University of California, Berkeley, CA 94720, USA

[2]California Institute for Quantitative Biosciences (QB3), University of California, Berkeley, CA 94720, USA

[3]Physical and Life Sciences Directorate, Lawrence Livermore National Laboratory, Livermore, CA 94550, USA

[4]College of Chemistry, University of California, Berkeley, CA 94720, USA

[5]Department of Molecular and Cell Biology, University of California, Berkeley, CA 94720, USA

[6]Division of Environmental Genomics and Systems Biology, Lawrence Berkeley National Laboratory, Berkeley, CA, USA

Correspondence: Sabeeha S. Merchant, sabeeha@berkeley.edu, +1 510 664-5154, 408B Stanley Hall, Berkeley, CA 94720-3220

Study Funding: This work was supported by The Gordon and Betty Moore Foundation Symbiosis in Aquatic Systems Initiative Investigator Award GBML9203 (https://doi.org/10.37807/GBMF9203), and the Lawrence Livermore National Laboratory µBiospheres Scientific Focus Area award SCW1039 from the DOE OBER Genomic Sciences Program. S.D. acknowledges support from NIH T32 Genetic Dissection of Cells and Organisms training grant 1T32GM132022-01.

ABSTRACT

Although the green alga *Chlamydomonas reinhardtii* has long served as a reference organism, few studies have interrogated its role as a primary producer in microbial interactions. Here, we quantitatively investigated *C. reinhardtii's* capacity to support a heterotrophic microbe using the established coculture system with *Mesorhizobium japonicum*, a vitamin B_{12}-producing α-proteobacterium. Using stable isotope probing and nanoscale secondary ion mass spectrometry (nanoSIMS), we tracked the flow of photosynthetic fixed carbon and consequent bacterial biomass synthesis under continuous and diurnal light with single-cell resolution. We found that more ^{13}C fixed by the alga was taken up by bacterial cells under continuous light, invalidating the hypothesis that the alga's fermentative degradation of starch reserves during the night would boost *M. japonicum* heterotrophy. $^{15}NH_4$ assimilation rates and changes in cell size revealed that *M. japonicum* cells reduced new biomass synthesis in coculture with the alga but continued to divide – a hallmark of nutrient limitation often referred to as reductive division. Despite this sign of starvation, the bacterium still synthesized vitamin B_{12} and supported the growth of a B_{12}-dependent *C. reinhardtii* mutant. Finally, we showed that bacterial proliferation could be supported solely by the algal lysis that occurred in coculture, highlighting the role of necromass in carbon cycling. Collectively, these results reveal the scarcity of fixed carbon in this microbial trophic relationship (particularly under environmentally relevant light regimes), demonstrate B_{12} exchange even during bacterial starvation, and underscore the importance of quantitative approaches for assessing metabolic coupling in algal-bacterial interactions.

KEY WORDS

rhizobia; chlorophyte; photoautotroph; diel; cobalamin; co-cultivation; symbiosis; SIP

46 **INTRODUCTION**

47 Photosynthetic microbes are responsible for a large fraction of the primary productivity
48 on our planet [1]. These organisms supply the microbial world with raw materials for life,
49 thereby shaping communities and driving carbon cycling [2, 3]. Through exudation, lysis, and
50 predation, photosynthetic microbes provide a variety of reduced carbon substrates with various
51 diffusion rates and accessibility to heterotrophic bacteria. The primary consumers recycle carbon
52 back to inorganic forms, closing the "microbial loop" that constitutes a major component of
53 biogeochemical carbon cycling [2, 4, 5]. Heterotrophic bacteria can also influence algal
54 productivity, for example, by changing the availability of critical micronutrients for algal growth
55 and metabolism [6–8].

56 The green alga *Chlamydomonas reinhardtii* has served as a reference organism for
57 discoveries in photosynthesis, cilia-based motility, and the eukaryotic cell cycle [9]. Extensive
58 work on axenic (bacteria-free) cultures has provided detailed knowledge of the pathways and
59 regulons for photosynthesis and primary metabolism. This chlorophyte has a flexible metabolic
60 repertoire, with the capacity to grow by photoautotrophy alone or by acetate assimilation. Under
61 diurnal cycles, *C. reinhardtii*'s metabolism is shaped by programmed waves of gene expression
62 that accommodate diurnal changes in light and oxygen availability in natural environments [10,
63 11]. Photosynthesis fuels cell growth and starch synthesis during the day, and starch reserves are
64 glycolytically degraded at night, providing a source of energy until the next dawn. Although
65 extensive knowledge of its metabolism makes *C. reinhardtii* an attractive model organism to
66 study microbial trophic interactions, relatively little is known about how *C. reinhardtii*
67 contributes to its environment and influences its neighbors in the microbial world.

68 In its natural soil context, *C. reinhardtii* is surrounded by other microbes that exchange

69 nutrients, compete for resources, and communicate with one another. *C. reinhardtii* can enrich
70 for particular heterotrophic bacteria from bulk soil, demonstrating that the alga's growth can
71 influence the metabolisms and behaviors of various bacteria [12, 13]. Studies of
72 *Chlamydomonas*-bacteria interactions have primarily focused on impacts to the alga's behavior,
73 in part due to technical challenges in probing bacterial physiology in mixed cultures. Bacteria are
74 known to supply vitamins and fixed nitrogen, facilitate iron assimilation, and impart thermal
75 tolerance to algal cultures [6, 7, 14–20]. Coculture of *C. reinhardtii* with various heterotrophic
76 bacteria (e.g. *Bradyrhizobium japonicum*, *Pseudomonas* spp.) has been shown to stimulate algal
77 H_2 production, starch accumulation, and viability under sulfur deprivation by consuming O_2 and
78 alleviating accumulation of fermentation byproducts from the medium [21]. Bacterial secondary
79 metabolites can also influence *C. reinhardtii*'s cell cycle and aggregation [22, 23]. In addition,
80 interactions between *C. reinhardtii* and vitamin B_{12}-producing rhizobia like *Mesorhizobium*
81 *japonicum* (previously referred to as *Mesorhizobium loti*), *Sinorhizobium meliloti*, and
82 *Rhizobium leguminosarum* have been used to study the evolution of vitamin dependency across
83 the algal tree of life [6, 15, 24–28]. *C. reinhardtii* does not require vitamin B_{12} for growth,
84 because it has retained a functional cobalamin-independent isoform of methionine synthase,
85 METE1. However, when vitamin B_{12} is supplied, *METE1* is repressed, and the vitamin is used as
86 a cofactor for the cobalamin-dependent isoform, METH1. When *C. reinhardtii* was grown in the
87 laboratory with a continuous supply of the vitamin, the alga acquired deleterious mutations in the
88 repressed *METE1* gene, yielding B_{12}-requiring strains (*mete1*) in less than 500 generations [25].
89 The interaction between the *C. reinhardtii mete1* mutant and *M. japonicum* is the most
90 well-studied *C. reinhardtii* coculture system. It has been suggested to be facultatively
91 mutualistic: the mutant alga receives the vitamin cofactor, and the bacterium is believed to

92 receive reduced carbon compounds that support heterotrophic growth. However, the mechanism
93 and magnitude of the flux of carbon transfer from *C. reinhardtii* to *M. japonicum* are unknown.
94 Quantitative investigations of algal-bacterial interactions have been challenging due to technical
95 barriers for studying eukaryotes and prokaryotes simultaneously. We have addressed this
96 challenge by using spatiotemporal stable isotope tracing via nanoscale secondary ion mass
97 spectrometry (nanoSIMS) to probe this simple model interaction – a technique which has
98 typically been used for studying complex polycultures from the field. We quantified the transfer
99 of fixed carbon from wild-type *C. reinhardtii* to *M. japonicum* in continuous and diurnal light.
100 Although some photosynthetically fixed carbon was taken up by the bacterial population, *M.*
101 *japonicum* growth was severely limited, resulting in reductive bacterial division. Thus, *C.*
102 *reinhardtii* primary productivity yields a low carrying capacity for this bacterium, particularly
103 under diurnal light. Nonetheless, *M. japonicum* provided adequate B_{12} to enable growth of the *C.*
104 *reinhardtii mete1* strain even when the bacterium itself exhibited signs of starvation. These
105 results highlight that in natural contexts, bacteria may not proliferate to the high cell densities
106 that are possible in nutrient-rich media often used in the laboratory, but they can still greatly
107 influence the metabolism and evolution of their neighbors in the microbial world.

108 **MATERIALS AND METHODS**

109 **Strains and culture conditions**

110 Three strains of *C. reinhardtii* were used in this study. The *mete1* strain generated
111 through experimental evolution on 1000 ng/l vitamin B_{12} [25] and its parental wild-type strain
112 were provided by Alison G. Smith (University of Cambridge, UK). According to its haplotype,
113 this strain is closely related to strain S24- (SI Fig. 1) [29]. For experiments testing the impact of
114 diurnal light, we used the cell-wall reduced strain CC-5390. This strain is amenable to

synchronization under diurnal cycles, providing a system with exceptional signal-to-noise for resolving diurnal patterns [10]. *M. japonicum* strain MAFF303099 was also provided by Alison G. Smith.

All experiments were performed in amended HSM minimal medium [30] with a modified trace element solution [31], 2 mM $MgSO_4 \cdot 7H_2O$, 10 µg/l biotin, and 10 µM $CoCl_2$ unless otherwise specified (Supplementary Data File S2: Media composition). Cultures were grown in either 250 ml Erlenmeyer flasks containing 100 ml medium and bubbled with filter-sterilized air (provided by an aquarium pump), 6-well plates with 3 ml medium, or 250 ml beakers with 50 ml medium. Algal cultures and cocultures were incubated at 28°C, agitated at 110–130 rpm, and illuminated with 200 µmol photons/m^2/s cool white light (Sylvania Dulux L55WFT55DL/841) continuously or under diurnal 12-h-light/12-h-dark cycles.

C. reinhardtii cells were precultivated axenically in photoautotrophic conditions for at least 3 passages prior to experiments. The *mete1* strain was precultivated with 200–250 ng/l vitamin B_{12} (cyanocobalamin). For experiments comparing coculture in continuous light versus diurnal light, *C. reinhardtii* CC-5390 cells were precultivated in flat-panel photobioreactors (Photon System Instruments, Drásov, Czechia) as previously described under the respective light regime to achieve adequate synchrony of the diurnal populations [10].

Bacterial cells were precultivated in 14 ml polystyrene round-bottom tubes with 3 ml amended HSM containing 0.2% sucrose, agitated at 200 rpm, and incubated at 28°C. When larger volumes were required for inoculation, cells were precultivated instead in 250 ml Erlenmeyer flasks containing 100 ml medium, continuously bubbled with air, and agitated at 110–130 rpm. Bacterial cells were collected by centrifugation at 8000 x*g* and washed three times in 0.85% NaCl to remove sucrose before use as inoculum. Optical density at 600 nm (OD_{600}) was

138 used to estimate the cell density of washed cell suspensions used for inoculation.

139 **Cell number, size, and cytotoxicity measurements**

140 *C. reinhardtii* cell density and size were determined using a hemocytometer and ImageJ
141 or a Beckman Coulter Multisizer 3 with a 50 µm orifice (Beckman Coulter, CA, USA). Bacterial
142 cell density was determined by counting colony forming units (CFU) in 10 µl spots of serial
143 dilutions on Typtone Yeast (TY) agar medium (Supplementary Data File S2: Media
144 composition) after 4 d of incubation at 30°C in the dark.

145 Algal cellular integrity was estimated using CellTox Green Cytotoxicity Assay (Promega,
146 WI, USA). *C. reinhardtii* sample densities were adjusted to $1x10^6$ cells/ml. Triplicate killed
147 control samples were prepared by heating cells at 90°C for 10 min. Fluorescence was measured
148 in a black-walled 96-well plate using a SpectraMax iD3 plate reader (Molecular Devices, CA,
149 USA). Background fluorescence of a medium blank was subtracted from all values. Results were
150 reported relative to killed control samples.

151 Samples for fluorescence microscopy were fixed overnight in 4% paraformaldehyde at
152 4°C in the dark. Fixed samples were then collected by centrifugation at 10,000 x*g*, washed in
153 phosphate buffered saline (PBS) (pH 7), and stored in 1:1 ethanol:PBS at -20°C. For imaging,
154 samples were spotted on 0.22 µm GTTP type isopore polycarbonate filters and washed with
155 sterile water to remove residual salts. Prepared filters were mounted on slides with 5 µg/ml
156 DAPI in Citifluor antifade mounting medium buffered with PBS and imaged using a Zeiss
157 Axioimager M2 microscope with a DAPI filter set (Ex 350/50, Em 460/50). Bacterial cell
158 lengths were measured manually using ImageJ Version 2.1.0/1.53c by drawing a line from one
159 pole of the cell to the other along the longer axis.

160 **Total organic carbon measurements**

161 Total nonpurgeable organic carbon content (NPOC) of cells was determined using a
162 TOC-L Shimadzu Total Organic Carbon Analyzer (Shimadzu, Kyoto, Japan). 10–40 ml culture
163 was collected by centrifugation at 8,000 x*g* for 2 min, and the supernatant was collected and then
164 stored at -20°C until analysis. Spent media were diluted 2-fold and HCl was added to 27 mM.
165 All samples were sparged to remove inorganic carbon. Some organic carbon may be purged from
166 the sample by this method, so we report "nonpurgeable" organic carbon.

167 **Stable isotope labelling and nanoSIMS**

168 $^{15}NH_4Cl$ (99% ^{15}N, Cambridge Isotope Laboratories, MA, USA) was provided directly in
169 the culture medium, replacing 50% of the NH_4Cl in HSM. 13 h after inoculation, $^{13}CO_2$ was
170 provided to cultures by bubbling air through a solution of $NaH^{13}CO_3$ (99% ^{13}C, Cambridge
171 Isotope Laboratories) and then into the cultures as previously described [32]. Killed controls
172 were generated by treating cells with 4% paraformaldehyde for 20 min in the dark. Coculture
173 experiments were otherwise conducted as described above.

174 For nanoSIMS analyses, samples were fixed and deposited on filters as described above
175 for fluorescence microscopy. Dry filter pieces were then mounted on 1 inch round stubs using
176 carbon tabs (Ted Pella, Inc., CA, USA) and gold coated. Data were collected on a NanoSIMS 50
177 (CAMECA, Gennevilliers, France) using a 1.5 pA Cs^+ primary ion beam. The secondary ion
178 masses of $^{12}C_2^-$, $^{12}C^{13}C^-$, $^{12}C^{14}N^-$, $^{12}C^{15}N^-$, and $^{32}S^-$ were collected. Raw nanoSIMS images were
179 processed using L'image (L. Nittler, Carnegie Institution of Washington, D.C., USA). Individual
180 cell regions of interest (ROIs) were manually circled using size and high $^{12}C^{14}N$ signal to
181 identify bacterial cells and high $^{12}C^{13}C$ signal along with the secondary electron image to identify
182 algal cells. Isotope enrichment in atom percent enrichment (APE) for $^{12}C^{13}C^-/^{12}C_2^-$ and $^{12}C^{15}N^-$
183 $/^{12}C^{14}N^-$ were calculated using standard ratios of 0.02247 and 0.00367, respectively. Enrichment

184 data are also presented as net assimilation (N_{net} and C_{net}). The fraction of newly synthesized
185 biomass relative to total biomass was calculated against an unlabeled biomass standard as
186 previously described [33]:

187 $$X_{net} = \frac{F_{cell} - F_{unlabelled}}{F_{substrate} - F_{unlabelled}}$$

188 Where *F* is the abundance of the heavy isotope (^{15}N or ^{13}C) over the total (^{14}N+^{15}N or ^{12}C+^{13}C,
189 respectively). For ^{15}N, net assimilation was calculated relative to the known isotopic composition
190 of the initial source substrate added to the medium. For ^{13}C, net bacterial assimilation was
191 calculated relative to the average algal biomass isotopic composition in the respective
192 experiment (continuous light or diurnal light) as a rough estimation of the source substrate.

193 **Vitamin B_{12} bioassay**

194 Vitamin B_{12} concentration was determined using the *Escherichia coli* B_{12} bioassay
195 described previously [34, 35]. The bioassay uses two *E. coli* strains: the Δ*metE*Δ*metH* control
196 strain requires methionine for growth, and the Δ*metE* strain can grow when provided either
197 methionine or B_{12}. The amount of B_{12} in a sample is determined by subtracting the growth of the
198 Δ*metE*Δ*metH* control strain from the growth of the Δ*metE* strain after 24 h incubation in the
199 sample and then comparing to a vitamin B_{12} standard curve.

200 Culture samples and vitamin B_{12} standards were boiled at 100°C for 10 min. Cell debris
201 was removed by centrifugation at 16,000 x*g* for 2 min, and the supernatants were snap frozen in
202 liquid N_2 and stored at -80°C until analysis. *E. coli* strains were precultivated twice in
203 polystyrene round-bottom tubes in 2 ml M9 medium (Supplementary Data File S2: Media
204 composition) with 0.2% glucose and 1 mg/ml methionine at 37°C and 250 rpm agitation for 24
205 h. *E. coli* inocula were then collected by centrifugation at 10,000 x*g* for 1 min and washed three
206 times with M9 medium prior to use in the bioassay. Samples and standards were thawed at room

207 temperature and diluted in 2X M9 medium with 0.4% glucose and water to a final volume of 2
208 ml in polystyrene round-bottom tubes, to which either the Δ*metE* strain or the Δ*metE*Δ*metH*
209 control strain was added to a starting density of 0.01 OD_{600}. The bioassay was then incubated at
210 37°C and agitated at 250 rpm for 24 h, and growth was measured by OD_{600}. Sample B_{12}
211 concentration was determined relative to a standard curve.

212 **Spent medium and cell lysate experiments**

213 Wild-type *C. reinhardtii* was grown for 48 h in continuous light until density reached 1–
214 $4x10^6$ cells/ml. Cells were collected by centrifugation in 500 ml polypropylene bottles for 4 min
215 at 11,900 x*g* and 4°C. The supernatant was passed through a 0.22 µm filter to generate sterile
216 spent medium. Cell pellets were resuspended in fresh medium to the original culture volume and
217 then sonicated using a Fisherbrand Model 505 Sonic Dismembrator (Fisher Scientific, PA, USA)
218 on ice for 45 min with alternating 10 s at 30% intensity and 15 s "off" steps. The supernatant of
219 the resulting cell lysate was then passed through a 0.22 µm filter to generate sterile soluble cell
220 lysate. Spent medium, soluble cell lysate, and parallel live *C. reinhardtii* cultures were then
221 inoculated with *M. japonicum* as described above, and growth was monitored over another 48 h.

222 To determine the bacterial growth supported by substrates in *C. reinhardtii* cell lysate
223 when these substrates are present at a relevant concentration, wild-type *C. reinhardtii* was grown
224 for 48 h in continuous light, and spent medium and soluble cell lysate were prepared as described
225 above. Then, the NPOC of the two culture fractions was measured, and the cell lysate was
226 diluted to the same NPOC concentration as the spent medium using fresh medium. 3 ml of the
227 diluted cell lysate was inoculated with *M. japonicum* as described above in parallel with spent
228 medium, fresh medium, and fresh medium with 150 µg/ml sucrose in polystyrene round-bottom
229 tubes. Cultures were incubated at 30°C and agitated at 200 rpm, and growth was monitored for

230 roughly 48 h.

231 **RESULTS**

232 ***M. japonicum* growth is severely limited in coculture with *C. reinhardtii*, especially under**

233 **diurnal light**

234 Previous work suggested that *C. reinhardtii* supports heterotrophic growth of the

235 rhizobial bacterium *M. japonicum* when cocultured in minimal medium given light and

236 atmospheric CO_2 [25, 26, 28, 36]. As a first step in characterizing the transfer of fixed carbon in

237 this relationship, we compared the growth of *M. japonicum* when incubated alone or together

238 with wild-type *C. reinhardtii* in minimal medium with either no exogenous carbon source or

239 with 150 µg/ml sucrose (Fig. 1). Coculture with the bacterium did not have a discernable impact

240 on *C. reinhardtii* growth or physiology (Fig. 1B, SI Fig. 2, $p > 0.05$). *M. japonicum* grew

241 considerably with sucrose and only marginally without it, but we found that coculture with *C.*

242 *reinhardtii* did not significantly increase the maximum bacterial density in either condition (Fig.

243 1C, $p > 0.05$). Although the maximum density of *M. japonicum* in coculture without sucrose

244 (~$3x10^7$–$5x10^8$ CFU/ml) was similar to what has been observed previously [28], we found that

245 the bacterium was able to achieve a comparable density without the alga, in contrast to previous

246 reports.

247 As the growth of *M. japonicum* was not significantly stimulated by wild-type *C.*

248 *reinhardtii*, it seemed that the alga did not supply adequate substrates for the bacterium's

249 heterotrophic metabolism under these conditions. This could be because *C. reinhardtii* released

250 fixed carbon compounds in insufficient quantities, or because *M. japonicum* is unable to

251 metabolize the specific compounds generated by *C. reinhardtii*. We had initially illuminated

252 cocultures with continuous light to maximize algal carbon fixation and growth rate, but we

253 hypothesized that the alga's nighttime metabolism could stimulate additional growth of *M.*
254 *japonicum*. During the day, the alga fixes carbon to build biomass and stores photosynthate as
255 starch [10]. After sufficient growth during the light phase, cells initiate DNA synthesis and
256 mitosis in the dark, followed by a G0 phase during which starch reserves are degraded by
257 glycolysis and genes for fermentation are expressed. Fermentation "waste products" released by
258 algae in the night could serve as a readily available source of fixed carbon for cooccurring
259 bacteria.

260 To test the impact of different light regimes on the interaction, we used the readily
261 synchronized *C. reinhardtii* strain CC-5390. Synchronized populations allow excellent temporal
262 separation of cells in distinct metabolic phases of the cell cycle, and could reveal a diurnal
263 pattern in bacterial growth resulting from the algal partner's diurnal metabolism. We compared
264 cocultures and monocultures under continuous and diurnal light over several days with high
265 temporal resolution. *C. reinhardtii*'s doubling time is slower under diurnal light (cells only
266 divide once per day), but we designed the experiment to achieve the same final amount of algal
267 biomass under the two light regimes. *C. reinhardtii* strain CC-5390 density reached roughly
268 $4x10^6$ cells/ml under all conditions (Fig. 2A, 2B). This was roughly 2X higher than the density
269 reached by the wild-type strain used in Fig. 1, although the strains appeared to reach stationary
270 phase in the same amount of time under continuous light (72 h). Algal growth was again
271 unaffected by the bacterium. In contrast, we found that *M. japonicum* density increased
272 significantly in the presence of CC-5390 under both light regimes (Fig. 2C–2E). CC-5390 may
273 support more growth of the bacterium than the wild-type strain because it is more prone to cell
274 lysis and releases more nonpurgeable organic carbon (NPOC) into the spent medium (SI Fig. 3).
275 However, we could not discern a clear temporal pattern in bacterial proliferation over the diurnal

276 cycles, and contrary to our hypothesis, we found that continuously illuminated cocultures
277 supported 3-fold more bacterial cells than did diurnally illuminated cocultures (Fig. 2E, p =
278 0.04). Spent medium from continuous light-grown *C. reinhardtii* had significantly more NPOC
279 than spent medium from diurnal light-grown *C. reinhardtii* of the same culture density,
280 suggesting that more dissolved organic carbon was available to the bacterium under continuous
281 light (Fig. 2F, $p < 0.05$). Algal cell lysis was similar under the two light regimes, so differences
282 in algal spent medium NPOC suggest that *C. reinhardtii* exudes more reduced carbon in
283 continuous light than in diurnal light (SI Fig. 4, $p > 0.05$). Finally, the presence of *M. japonicum*
284 did not significantly reduce the concentration of NPOC in the spent medium (Fig. 2F, Student's
285 *t*-test, $p > 0.05$). This could mean that either *M. japonicum* did not take up significant amounts of
286 organic carbon from the medium or that it could not fully oxidize it to CO_2, and instead released
287 reduced carbon waste products back into the extracellular milieu.

288 **Stable isotope probing reveals mismatch between bacterial biomass synthesis and division**
289 **in coculture**

290 To determine the amount of carbon fixed by *C. reinhardtii* that is taken up by *M.*
291 *japonicum*, we conducted stable isotope probing experiments using $^{13}CO_2$. Cocultures of CC-
292 5390 and *M. japonicum* grown under continuous and diurnal light as in Fig. 2 were bubbled with
293 air containing $^{13}CO_2$. $^{15}NH_4Cl$ was added to the medium as an independent tracer of biomass
294 synthesis, complementing measurements of cell density. We assayed label uptake with single-
295 cell resolution using nanoSIMS.

296 We found substantial ^{13}C enrichment of the algal cells, which remained at a similar
297 concentration throughout the timepoints examined (Fig. 3A, SI Fig. 5, SI Fig. 6). In addition, we
298 observed ^{13}C enrichment of bacterial cells, which increased with time in cocultures under both

299 light regimes (Fig. 3A, SI Fig. 5, SI Fig. 6, $p < 0.05$). Killed controls and monocultures of *M.*
300 *japonicum* on various substrates demonstrated that this enrichment was not a result of
301 nonspecific background or direct CO_2 incorporation by the bacterium (i.e. through anapleurotic
302 carboxylation reactions) (SI Fig. 6, SI Fig. 7). Thus, a meaningful amount of carbon derived
303 from algal photoautotrophy was in fact incorporated into *M. japonicum* biomass in the
304 cocultures.

305 We compared the extent of carbon transfer under continuous and diurnal light by
306 calculating the fraction of bacterial carbon that was derived from algal carbon, C_{net}, using the
307 average ^{13}C content of algal biomass over the course of each experiment as a rough measure of
308 the source carbon isotopic composition. We found that significantly more algal ^{13}C was
309 transferred to bacterial cells under continuous light over 48 h (0.17 median C_{net} in continuous
310 light, 0.09 median C_{net} in diurnal light) (Fig. 3B, $p = 6x10^{-6}$). This was consistent with our
311 observation that spent medium NPOC and *M. japonicum* cell density were greater in cocultures
312 exposed to continuous light than those exposed to diurnal light (Fig. 2, SI Fig. 8A).

313 Both the ^{13}C and ^{15}N enrichment in *M. japonicum* cells were lower than we had expected
314 from the increase in bacterial CFUs observed in the experiment (>3-fold increase in CFUs during
315 the first 24 h of coculture under continuous light), suggesting a mismatch between the change in
316 cell density and the bacterial biomass synthesized (Fig. 3C, SI Fig. 8A). We quantified the
317 magnitude of this mismatch using the ^{15}N label, for which the source isotopic composition was
318 better constrained, as opposed to that of the ^{13}C label which was delivered in the gas phase in an
319 open system. Using the source ^{15}N composition and the measured isotopic composition of
320 bacterial cells at each timepoint, we calculated the fraction of newly synthesized biomass
321 generated from the source substrate over the course of the experiment: N_{net} [33]. We compared

322 this to the expected N_{net} that would be observed if each doubling in CFUs in the culture occurred
323 upon a doubling in bacterial biomass (0.99 N_{net} for cells grown on sucrose after 8–13 doublings,
324 0.63–0.97 N_{net} for cells co-cultivated with *C. reinhardtii* after 1–5 doublings) (SI Fig. 8B).
325 Indeed, the measured N_{net} of *M. japonicum* cells in the cocultures was much lower than the
326 expected values at all measured timepoints (0.18–0.34 N_{net}), whereas the measured values
327 matched the expected values during logarithmic-phase growth on sucrose (Fig. 4A). This showed
328 that in coculture with *C. reinhardtii*, *M. japonicum* cells reduced new biomass synthesis by 24 h
329 and yet continued to divide – a hallmark of bacterial starvation often referred to as reductive
330 division [37–39]. As nutrients available for a bacterium's growth decrease, the cell volume
331 added prior to cell division is reduced, leading to smaller daughter cells [40–43].
332 If the deviation of the observed N_{net} from the expected N_{net} indeed reflected reductive
333 division, bacterial cells in the coculture would be smaller than cells in the logarithmic phase of
334 growth on sucrose, which are typically 2 µm in length. When we measured the size of the
335 bacterial cells, we found that *M. japonicum* cells were indeed smaller in the cocultures: mean cell
336 length was 1.4–1.5 µm after 24 h in coculture, whereas it was 2.3 µm after 24 h of growth on
337 sucrose (Fig. 4B, 4C). When sucrose was presumably depleted from the medium over the
338 subsequent day in the monoculture, mean cell length decreased to a similar extent, demonstrating
339 that reductive division occurs upon carbon limitation in *M. japonicum*.
340 Taken together, these data show that photosynthetically fixed carbon was indeed
341 transferred from *C. reinhardtii* to *M. japonicum* under both continuous and diurnal light, and that
342 although this amount was not sufficient for balanced logarithmic-phase growth of the bacterium,
343 it allowed for a small amount of bacterial proliferation.
344 **Reductively dividing bacteria still deliver sufficient vitamin B_{12} to support growth of the**

345 **B_{12}-requiring *mete1* strain**

346 As reductive division had not previously been reported in the *C. reinhardtii-M.*
347 *japonicum* interaction, we wondered whether the phenomenon also occurs during coculture with
348 the B_{12}-requiring *mete1* strain of *C. reinhardtii*, and if so, whether the bacterium still synthesizes
349 adequate B_{12} to support the mutant's growth. We compared the change in bacterial cell size after
350 growth on 150 µg/ml sucrose to changes during coculture with either wild-type *C. reinhardtii* or
351 *mete1*. In all conditions, we observed a 37–50% reduction in *M. japonicum* cell length over 54 h
352 of cultivation (Fig. 5A, 5B). This suggested that bacterial carbon limitation occurs to a similar
353 extent during coculture with the *mete1* strain as with the wild type.

354 To test whether reductively dividing *M. japonicum* still delivers vitamin B_{12} to *C.*
355 *reinhardtii*, we compared the growth of the *C. reinhardtii mete1* strain in coculture and
356 monoculture without exogenous B_{12}, and we monitored changes in vitamin B_{12} concentration
357 overtime using a bioassay [34, 35]. *mete1* growth was limited by B_{12} relative to the wild-type *C.*
358 *reinhardtii*, but the B_{12}-requiring strain grew significantly more in the presence of *M. japonicum*
359 despite reductive bacterial division (Fig. 5C, 5E, $p < 0.05$). Furthermore, we found that *M.*
360 *japonicum* produced significant vitamin B_{12} in coculture, but only after 24 h (Fig. 5F, $p < 0.05$),
361 even though bacterial biomass synthesis and cell size have decreased substantially by that time
362 (Fig. 4). This demonstrates that bacterial B_{12} synthesis and sharing occur despite the carbon
363 limitation experienced during the trophic interaction with the alga.

364 Although there were roughly 10X more *C. reinhardtii* cells present in the wild-type
365 coculture than the B_{12}-limited mutant coculture, there was no difference in *M. japonicum* density
366 between these two conditions (Fig. 5D, $p > 0.05$). Thus, greater algal density does not translate
367 into greater *M. japonicum* growth, as noted previously [28]. We observed this phenomenon in

368 cocultures inoculated at several starting relative abundances (SI Fig. 10). This suggests that
369 carbon transfer from the alga to the bacterium could be indirect.

370 ***C. reinhardtii* lysis can explain observed *M. japonicum* proliferation in coculture**

371 To distinguish the source of the fixed carbon that supports *M. japonicum* proliferation in
372 coculture, we compared *M. japonicum* growth with live *C. reinhardtii* to growth in *C. reinhardtii*
373 spent medium and in the soluble fraction of *C. reinhardtii* cell lysate. Spent medium supported
374 the same number of *M. japonicum* cells as did coculture, demonstrating that the observed
375 increase does not require a direct interaction with the alga (Fig. 6A). Cell lysate from *C.*
376 *reinhardtii* supported almost an order of magnitude more *M. japonicum* proliferation. Therefore,
377 we hypothesized that the fixed carbon transferred in our cocultures could be sourced from a few
378 lysed *C. reinhardtii* cells rather than from photosynthate exuded by live algal cells.

379 Having determined the increase in viable *M. japonicum* cells supported by lysate from a
380 known density of *C. reinhardtii* cells (1.7×10^8 CFU/ml on average after 48 h in lysate from
381 1.6×10^6 *C. reinhardtii* cells/ml culture), we estimated the theoretical increase in *M. japonicum*
382 CFUs supported by a single lysed *C. reinhardtii* cell to be 100±43 CFU in 48 h. From that, we
383 estimated how many *C. reinhardtii* cells would have to lyse in the coculture to enable the *M.*
384 *japonicum* proliferation observed: roughly 1.1×10^5 *C. reinhardtii* cells/ml, which corresponds to
385 1.8% of the *C. reinhardtii* populations in those cocultures. To test the actual degree of algal lysis
386 in our cultures, we measured algal cellular integrity using the CellTox Green Cytotoxicity Assay.
387 This assay uses a membrane-impermeable DNA dye, resulting in fluorescence from cells whose
388 plasma membrane has been compromised or from extracellular DNA [44]. We compared live
389 culture fluorescence to killed control samples and found that 1–3% of the wild-type *C.*
390 *reinhardtii* population had compromised cellular integrity (Fig. 6B). Thus, the fraction of dead or

391 dying *C. reinhardtii* cells measured by this assay is comparable to that needed to explain the
392 observed *M. japonicum* proliferation.

393 Finally, we reasoned that if *M. japonicum* is primarily growing on algal cell lysate, then
394 cell lysate should support the same amount of bacterial proliferation as spent medium when
395 present at the same organic carbon content. Thus, we compared *M. japonicum* growth in spent
396 medium and diluted cell lysate from wild-type *C. reinhardtii* when both were present at roughly
397 15 µg/ml NPOC. Indeed, algal cell lysate alone supported the same *M. japonicum* growth as
398 spent medium when present at a relevant concentration: bacterial cell density was not
399 significantly different between these two conditions at most timepoints examined (Fig. 6C, $p >$
400 0.05). The slight increase in *M. japonicum* density in the diluted cell lysate condition could be
401 attributed to increased availability of micronutrients in the fresh medium used to dilute the algal
402 cell lysate. Taken together, these data are consistent with the interpretation that *M. japonicum*
403 growth in coculture is enabled by substrates that are released through *C. reinhardtii* cell lysis
404 rather than by substrates exuded by live *C. reinhardtii* cells.

405 **DISCUSSION**

406 Most studies of symbioses between *C. reinhardtii* and heterotrophic bacteria to date have
407 focused on impacts on the alga, leaving open the question of how this model phototroph might
408 influence bacterial growth and physiology. Here, we have investigated *C. reinhardtii's* role as a
409 primary producer in the established coculture system with *M. japonicum*. We have tied carbon
410 cycling in the interaction to alterations in bacterial growth and physiology through quantitative,
411 single-cell analyses. Under continuous light, we found that the alga increased the number of
412 viable bacterial cells, albeit marginally so. We tested whether nighttime metabolism might
413 increase the alga's propensity for carbon sharing, but we found that diurnal illumination actually

414 decreased the productivity of the partnership. Using nanoSIMS to visualize ^{13}C enrichment with
415 high spatial resolution, we quantitatively demonstrated transfer of carbon fixed by the model alga
416 to the bacterium. Roughly 17% of the carbon in *M. japonicum* cells was derived from *C.*
417 *reinhardtii* over 36 h under continuous light, whereas only ~9% of the *M. japonicum* carbon
418 came from *C. reinhardtii* over the same amount of time under diurnal light. Bulk measurements
419 showed that algal cultures of similar densities had more organic carbon in their spent medium
420 after continuous illumination than after diurnal illumination. Together, these results suggest that
421 the increased metabolic rate realized under continuous light may be more beneficial for *M.*
422 *japonicum* (and potentially other bacteria) than fermentative catabolism of starch presumed to
423 occur during the night. It is also possible that although *C. reinhardtii* expresses genes for
424 fermentative metabolism in the night, fermentative metabolites may not actually accumulate to
425 high enough levels in culture unless cells experience anoxia.

426 With *C. reinhardtii* as the sole source of fixed carbon, *M. japonicum* exhibited signs of
427 starvation, even under continuous light, highlighting the meagerness of the microbial trophic
428 relationship. The quantitative stable isotope probing experiments revealed that during coculture
429 with *C. reinhardtii*, *M. japonicum* synthesized significantly less biomass than expected given the
430 increase in viable bacterial cells. By direct measurement, we showed that *M. japonicum* divided
431 into small daughter cells within 24 h of carbon limitation in coculture, a physiological change
432 often referred to as reductive division. It is well known that as nutrients become limiting,
433 bacterial size at birth and the amount of cell volume each bacterium adds prior to division
434 decrease [40–43]. Studies on freshwater and marine bacteria have documented up to 90%
435 reduction in cell volume during carbon limitation [45–48]. This phenomenon is often considered
436 an adaptive strategy by which diverse bacteria survive starvation [37–39, 49]. By increasing cell

437 number and reducing cell volume, bacteria increase the probability that a member of the
438 population will encounter sufficient nutrients again and increase their surface area-to-volume
439 ratio to improve nutrient uptake. Reductively dividing cells also exhibit changes in stress
440 resistance and macromolecule synthesis. However, we found that despite its apparent starvation,
441 *M. japonicum* provided enough vitamin B_{12} to support a B_{12}-dependent *C. reinhardtii* mutant.
442 Vitamin supply enables growth of auxotrophs, influences gene expression and metabolism, and
443 can even give rise to vitamin dependency in algae [25, 50]. Thus, our results suggest that even
444 under austere conditions with meager supply of growth substrates, bacteria can still influence
445 algal physiology and evolution.

446 We also found that a direct interaction with *C. reinhardtii* was not required to achieve the
447 *M. japonicum* proliferation observed in coculture: growth in algal spent medium yielded the
448 same maximum density of viable *M. japonicum* cells as did coculture. Furthermore,
449 mechanically lysed *C. reinhardtii* cells yielded considerably higher *M. japonicum* densities. This
450 observation led us to hypothesize that perhaps this bacterium does not metabolize the exudates of
451 live *C. reinhardtii* cells at all. Instead, perhaps the small amount of bacterial growth observed in
452 coculture and in spent medium is due to the lysis of a small fraction of algal cells. It has long
453 been appreciated that even during rapid exponential growth, microbial cultures experience a
454 small death rate [51]. Furthermore, cell lysis is an important mechanism of nutrient transfer in
455 natural environments, and microbial necromass is a major component of the soil organic carbon
456 pool [52, 53]. For the experimental conditions examined here, we showed that ~2% of the *C.*
457 *reinhardtii* population in our cultures are present as necromass. Based on the *M. japonicum*
458 growth yields achieved in mechanically lysed *C. reinhardtii* cells, we calculated that this is
459 almost exactly the amount of algal necromass required to explain the *M. japonicum* proliferation

460 that occurred in coculture. When present at the same organic carbon concentration, algal cell
461 lysate supported the same amount of *M. japonicum* growth as algal spent medium. Therefore, we
462 propose that lysis is the primary mechanism of trophic transfer in this coculture system, rather
463 than exudation or direct exchange.

464 Given that very little growth of *M. japonicum* was observed from an interaction with *C.*
465 *reinhardtii* – even under conditions optimized for algal productivity – our results may suggest
466 that this model alga exhibits a low carrying capacity for heterotrophic bacteria in the
467 environment. Similar bacterial densities have been reported for other *C. reinhardtii* cocultures in
468 minimal media, including those with *Methylobacterium aquaticum* [54, 55]. However, it is
469 possible that other bacteria, such as those that may have co-evolved with *C. reinhardtii* in its
470 native environment, may possess greater capacity to metabolize compounds that *C. reinhardtii*
471 releases during growth. In addition, other bacteria may achieve greater access to growth
472 substrates through chemotaxis, interspecies signaling and direct exchange, or algicidal activity
473 [3, 56–59]. The mode of cell lysis (i.e. mechanical vs. viral) could also greatly impact the algal-
474 derived nutrients released to cooccurring heterotrophs [60]. Nonetheless, stable isotope probing
475 experiments on other algal-bacterial interactions and on seawater microbial communities have
476 reported similar levels of trophic carbon transfer to those we observed here [56, 61, 62]. This
477 suggests that although *C. reinhardtii* and *M. japonicum* may not commonly encounter one
478 another in nature, this relationship may be representative of naturally occurring microbial
479 phototroph-heterotroph interactions. Studying this model system has revealed important aspects
480 of microbial ecology, and our quantitative approach can serve as a roadmap for the future work
481 necessary to understand *C. reinhardtii*'s full potential as a primary producer in the microbial
482 world.

ACKNOWLEDGMENTS

This work was supported by The Gordon and Betty Moore Foundation Symbiosis in Aquatic Systems Initiative Investigator Award GBML9203 (https://doi.org/10.37807/GBMF9203), and the Lawrence Livermore National Laboratory µBiospheres Scientific Focus Area award SCW1039 from the DOE OBER Genomic Sciences Program. S.D. acknowledges support from NIH T32 Genetic Dissection of Cells and Organisms training grant 1T32GM132022-01. We thank Dr. Alison G. Smith and her group at the University of Cambridge for providing strains and for their generous discussions with us. We thank Dr. Michiko E. Taga at UC Berkeley for her guidance on the work. We thank Dr. Denise Schichnes and the UC Berkeley Biological Imaging Facility for fluorescence microscopy support. We also thank Christina Ramon at Lawrence Livermore National Laboratory and Charles Perrino at UC Berkeley for analytical support.

COMPETING INTERESTS

The authors declare no competing financial interests.

DATA AVAILABILITY

All data underlying this article are available in Supplementary Data File S1.

REFERENCES

1. Field CB, Behrenfeld MJ, Randerson JT, Falkowski P. Primary production of the biosphere: Integrating terrestrial and oceanic components. *Science (1979)* 1998; **281**: 237–240.
2. Azam F, Fenchel T, Field J, Gray J, Meyer-Reil L, Thingstad F. The ecological role of water-column microbes in the sea. *Mar Ecol Prog Ser* 1983; **10**: 257–263.

505 3. Seymour JR, Amin SA, Raina J-B, Stocker R. Zooming in on the phycosphere: the
506 ecological interface for phytoplankton–bacteria relationships. *Nat Microbiol* 2017; **2**:
507 17065.
508 4. Pomeroy LR. The ocean's food web, a changing paradigm. *Bioscience* 1974; **24**: 499–504.
509 5. Azam F, Malfatti F. Microbial structuring of marine ecosystems. *Nat Rev Microbiol* 2007;
510 **5**: 782–791.
511 6. Croft MT, Lawrence AD, Raux-Deery E, Warren MJ, Smith AG. Algae acquire vitamin
512 B_{12} through a symbiotic relationship with bacteria. *Nature* 2005; **438**: 90–93.
513 7. Amin SA, Green DH, Hart MC, Küpper FC, Sunda WG, Carrano CJ. Photolysis of iron–
514 siderophore chelates promotes bacterial–algal mutualism. *Proceedings of the National*
515 *Academy of Sciences* 2009; **106**: 17071–17076.
516 8. Hom EFY, Aiyar P, Schaeme D, Mittag M, Sasso S. A chemical perspective on
517 microalgal-microbial interactions. *Trends Plant Sci* 2015; **20**: 689–693.
518 9. Salomé PA, Merchant SS. A series of fortunate events: Introducing Chlamydomonas as a
519 reference organism. *Plant Cell* 2019; **31**: 1682–1707.
520 10. Strenkert D, Schmollinger S, Gallaher SD, Salomé PA, Purvine SO, Nicora CD, et al.
521 Multiomics resolution of molecular events during a day in the life of Chlamydomonas.
522 *Proceedings of the National Academy of Sciences* 2019; **116**: 2374–2383.
523 11. Zones JM, Blaby IK, Merchant SS, Umen JG. High-resolution profiling of a synchronized
524 diurnal transcriptome from *Chlamydomonas reinhardtii* reveals continuous cell and
525 metabolic differentiation. *Plant Cell* 2015; **27**: 2743–2769.

526 12. Durán P, Flores-Uribe J, Wippel K, Zhang P, Guan R, Melkonian B, et al. Shared features
527 and reciprocal complementation of the Chlamydomonas and Arabidopsis microbiota. *Nat*
528 *Commun* 2022; **13**: 406.
529 13. Kim B-H, Ramanan R, Cho D-H, Oh H-M, Kim H-S. Role of Rhizobium, a plant growth
530 promoting bacterium, in enhancing algal biomass through mutualistic interaction. *Biomass*
531 *Bioenergy* 2014; **69**: 95–105.
532 14. Lőrincz Z, Preininger É, Kósa A, Pónyi T, Nyitrai P, Sarkadi L, et al. Artificial tripartite
533 symbiosis involving a green alga (Chlamydomonas), a bacterium (Azotobacter) and a
534 fungus (Alternaria): Morphological and physiological characterization. *Folia Microbiol*
535 *(Praha)* 2010; **55**: 393–400.
536 15. Xie B, Bishop S, Stessman D, Wright D, Spalding MH, Halverson LJ. *Chlamydomonas*
537 *reinhardtii* thermal tolerance enhancement mediated by a mutualistic interaction with
538 vitamin B_{12}-producing bacteria. *ISME J* 2013; **7**: 1544–1555.
539 16. Amin SA, Parker MS, Armbrust EV. Interactions between diatoms and bacteria.
540 *Microbiology and Molecular Biology Reviews* 2012; **76**: 667–684.
541 17. Gobler C, Norman C, Panzeca C, Taylor G, Sañudo-Wilhelmy S. Effect of B-vitamins
542 (B_1, B_{12}) and inorganic nutrients on algal bloom dynamics in a coastal ecosystem. *Aquatic*
543 *Microbial Ecology* 2007; **49**: 181–194.
544 18. Sañudo-Wilhelmy SA, Gobler CJ, Okbamichael M, Taylor GT. Regulation of
545 phytoplankton dynamics by vitamin B_{12}. *Geophys Res Lett* 2006; **33**: L04604.
546 19. Helliwell KE. The roles of B vitamins in phytoplankton nutrition: new perspectives and
547 prospects. *New Phytologist* 2017; **216**: 62–68.

548 20. Keshtacher-Liebso E, Hadar Y, Chen Y. Oligotrophic bacteria enhance algal growth under
549 iron-deficient conditions. *Appl Environ Microbiol* 1995; **61**: 2439–41.
550 21. Fakhimi N, Gonzalez-Ballester D, Fernández E, Galván A, Dubini A. Algae-bacteria
551 consortia as a strategy to enhance H_2 production. *Cells* 2020; **9**: 1353.
552 22. Krespach MKC, Stroe MC, Flak M, Komor AJ, Nietzsche S, Sasso S, et al. Bacterial
553 marginolactones trigger formation of algal gloeocapsoids, protective aggregates on the
554 verge of multicellularity. *Proceedings of the National Academy of Sciences* 2021; **118**.
555 23. Windler M, Stuart R, Deutzmann JS, Mayali X, Navid A, D'haeseleer P, et al. Bacterial
556 exometabolites influence *Chlamydomonas* cell cycle and double algal productivity. *FEMS*
557 *Microbiol Ecol* 2022; **98**.
558 24. Kazamia E, Czesnick H, Nguyen TT Van, Croft MT, Sherwood E, Sasso S, et al.
559 Mutualistic interactions between vitamin B_{12}-dependent algae and heterotrophic bacteria
560 exhibit regulation. *Environ Microbiol* 2012; **14**: 1466–1476.
561 25. Helliwell KE, Collins S, Kazamia E, Purton S, Wheeler GL, Smith AG. Fundamental shift
562 in vitamin B_{12} eco-physiology of a model alga demonstrated by experimental evolution.
563 *ISME J* 2015; **9**: 1446–1455.
564 26. Bunbury F, Helliwell KE, Mehrshahi P, Davey MP, Salmon DL, Holzer A, et al.
565 Responses of a newly evolved auxotroph of Chlamydomonas to B_{12} deprivation. *Plant*
566 *Physiol* 2020; **183**: 167–178.
567 27. Helliwell KE, Scaife MA, Sasso S, Araujo APU, Purton S, Smith AG. Unraveling vitamin
568 B_{12} -responsive gene regulation in algae. *Plant Physiol* 2014; **165**: 388–397.

569 28. Bunbury F, Deery E, Sayer AP, Bhardwaj V, Harrison EL, Warren MJ, et al. Exploring
570 the onset of B_{12}-based mutualisms using a recently evolved *Chlamydomonas* auxotroph
571 and B_{12}-producing bacteria. *Environ Microbiol* 2022; **24**: 3134–3147.
572 29. Gallaher SD, Fitz-Gibbon ST, Glaesener AG, Pellegrini M, Merchant SS.
573 Chlamydomonas genome resource for laboratory strains reveals a mosaic of sequence
574 variation, identifies true strain histories, and enables strain-specific studies. *Plant Cell*
575 2015; **27**: 2335–2352.
576 30. Sueoka N. Mitotic replication of deoxynucleic acid in *Chlamydomonas reinhardi*.
577 *Proceedings of the National Academy of Sciences* 1960; **46**: 83–91.
578 31. Kropat J, Hong-Hermesdorf A, Casero D, Ent P, Castruita M, Pellegrini M, et al. A
579 revised mineral nutrient supplement increases biomass and growth rate in
580 *Chlamydomonas reinhardtii*. *The Plant Journal* 2011; **66**: 770–780.
581 32. Lingappa UF, Dupuis S, Mayali X, Merchant SS. Isotopically labelled inorganic carbon
582 delivered to algal cultures via bubbler bottle. *protocols.io* 2023.
583 33. Dekas AE, Parada AE, Mayali X, Fuhrman JA, Wollard J, Weber PK, et al.
584 Characterizing chemoautotrophy and heterotrophy in marine archaea and bacteria with
585 single-cell multi-isotope nanoSIP. *Front Microbiol* 2019; **10**.
586 34. Mok KC, Hallberg ZF, Taga ME. Purification and detection of vitamin B_{12} analogs. 2022.
587 pp 61–85.
588 35. Dupuis S, Schmollinger S, Merchant SS. Quantitative detection of vitamin B_{12} in algae by
589 bioassay and ICP-MS/MS. *protocols.io* 2022.

590 36. Laeverenz Schlogelhofer H, Peaudecerf FJ, Bunbury F, Whitehouse MJ, Foster RA, Smith
591 AG, et al. Combining SIMS and mechanistic modelling to reveal nutrient kinetics in an
592 algal-bacterial mutualism. *PLoS One* 2021; **16**: e0251643.
593 37. Thorne SH, Williams HD. Adaptation to nutrient starvation in *Rhizobium leguminosarum*
594 *bv. phaseoli*: analysis of survival, stress resistance, and changes in macromolecular
595 synthesis during entry to and exit from stationary phase. *J Bacteriol* 1997; **179**: 6894–
596 6901.
597 38. Shimaya T, Okura R, Wakamoto Y, Takeuchi KA. Scale invariance of cell size
598 fluctuations in starving bacteria. *Commun Phys* 2021; **4**: 238.
599 39. Bergkessel M, Delavaine L. Diversity in starvation survival strategies and outcomes
600 among heterotrophic proteobacteria. *Microb Physiol* 2021; **31**: 146–162.
601 40. Schaechter M, Maaløe O, Kjeldgaard NO. Dependency on medium and temperature of
602 cell size and chemical composition during balanced growth of *Salmonella typhimurium*. *J*
603 *Gen Microbiol* 1958; **19**: 592–606.
604 41. Vadia S, Levin PA. Growth rate and cell size: a re-examination of the growth law. *Curr*
605 *Opin Microbiol* 2015; **24**: 96–103.
606 42. Campos M, Surovtsev IV, Kato S, Paintdakhi A, Beltran B, Ebmeier SE, et al. A constant
607 size extension drives bacterial cell size homeostasis. *Cell* 2014; **159**: 1433–1446.
608 43. Taheri-Araghi S, Bradde S, Sauls JT, Hill NS, Levin PA, Paulsson J, et al. Cell-size
609 control and homeostasis in bacteria. *Current Biology* 2015; **25**: 385–391.
610 44. Haire TC, Bell C, Cutshaw K, Swiger B, Winkelmann K, Palmer AG. Robust microplate-
611 based methods for culturing and *in vivo* phenotypic screening of *Chlamydomonas*
612 *reinhardtii*. *Front Plant Sci* 2018; **9**.

613 45. Vrede K, Heldal M, Norland S, Bratbak G. Elemental composition (C, N, P) and cell
614 volume of exponentially growing and nutrient-limited bacterioplankton. *Appl Environ*
615 *Microbiol* 2002; **68**: 2965–71.
616 46. Troussellier M, Bouvy M, Courties C, Dupuy C. Variation of carbon content among
617 bacterial species under starvation condition. *Aquatic Microbial Ecology* 1997; **13**: 113–
618 119.
619 47. Holmquist L, Kjelleberg S. Changes in viability, respiratory activity and morphology of
620 the marine Vibrio sp. strain S14 during starvation of individual nutrients and subsequent
621 recovery. *FEMS Microbiol Ecol* 1993; **12**: 215–223.
622 48. Mårdén P, Tunlid A, Malmcrona-Friberg K, Odham G, Kjelleberg S. Physiological and
623 morphological changes during short term starvation of marine bacterial islates. *Arch*
624 *Microbiol* 1985; **142**: 326–332.
625 49. Nyström T, Larsson C, Gustafsson L. Bacterial defense against aging: role of the
626 *Escherichia coli* ArcA regulator in gene expression, readjusted energy flux and survival
627 during stasis. *EMBO J* 1996; **15**: 3219–28.
628 50. Sokolovskaya OM, Shelton AN, Taga ME. Sharing vitamins: Cobamides unveil microbial
629 interactions. *Science* 2020; **369**.
630 51. Kelly CD, Rahn O. The growth rate of individual bacterial cells. *J Bacteriol* 1932; **23**:
631 147–153.
632 52. Gude S, Pherribo GJ, Taga ME. Emergence of metabolite provisioning as a by-product of
633 evolved biological functions. *mSystems* 2020; **5**.

634 53. Sokol NW, Slessarev E, Marschmann GL, Nicolas A, Blazewicz SJ, Brodie EL, et al. Life
635 and death in the soil microbiome: how ecological processes influence biogeochemistry.
636 *Nat Rev Microbiol* 2022; **20**: 415–430.
637 54. Ban S, Lin W, Wu F, Luo J. Algal-bacterial cooperation improves algal photolysis-
638 mediated hydrogen production. *Bioresour Technol* 2018; **251**: 350–357.
639 55. Calatrava V, Hom EFY, Llamas Á, Fernández E, Galván A. OK, thanks! A new
640 mutualism between Chlamydomonas and methylobacteria facilitates growth on amino
641 acids and peptides. *FEMS Microbiol Lett* 2018; **365**.
642 56. Samo TJ, Kimbrel JA, Nilson DJ, Pett-Ridge J, Weber PK, Mayali X. Attachment
643 between heterotrophic bacteria and microalgae influences symbiotic microscale
644 interactions. *Environ Microbiol* 2018; **20**: 4385–4400.
645 57. Jackrel SL, Yang JW, Schmidt KC, Denef VJ. Host specificity of microbiome assembly
646 and its fitness effects in phytoplankton. *ISME J* 2021; **15**: 774–788.
647 58. Aiyar P, Schaeme D, García-Altares M, Carrasco Flores D, Dathe H, Hertweck C, et al.
648 Antagonistic bacteria disrupt calcium homeostasis and immobilize algal cells. *Nat*
649 *Commun* 2017; **8**: 1756.
650 59. Raina J-B, Giardina M, Brumley DR, Clode PL, Pernice M, Guagliardo P, et al.
651 Chemotaxis increases metabolic exchanges between marine picophytoplankton and
652 heterotrophic bacteria. *Nat Microbiol* 2023; **8**: 510–521.
653 60. Pherribo GJ, Taga ME. Bacteriophage-mediated lysis supports robust growth of amino
654 acid auxotrophs. *ISME J* 2023; **17**: 1785–1788.

655 61. Arandia-Gorostidi N, Weber PK, Alonso-Sáez L, Morán XAG, Mayali X. Elevated
656 temperature increases carbon and nitrogen fluxes between phytoplankton and
657 heterotrophic bacteria through physical attachment. *ISME J* 2017; **11**: 641–650.
658 62. de-Bashan LE, Mayali X, Bebout BM, Weber PK, Detweiler AM, Hernandez J-P, et al.
659 Establishment of stable synthetic mutualism without co-evolution between microalgae and
660 bacteria demonstrated by mutual transfer of metabolites (NanoSIMS isotopic imaging)
661 and persistent physical association (Fluorescent *in situ* hybridization). *Algal Res* 2016; **15**:
662 179–186.
663

FIGURES

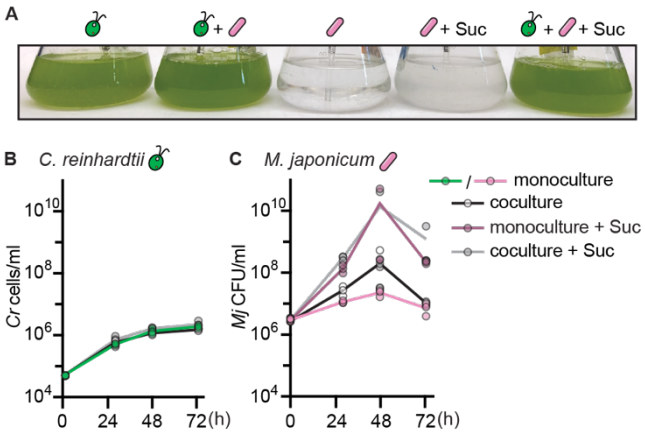

Figure 1: Wild-type *C. reinhardtii* does not significantly improve growth of *M. japonicum*. Triplicate cultures (n = 3) were inoculated with or without 150 µg/ml sucrose and maintained under continuous light, bubbled with air, and shaken at 110 rpm. (A) Representative image of cultures 72 h after inoculation. (B) Wild-type *C. reinhardtii* cell density in cultures over time after inoculation. (C) *M. japonicum* cell density in cultures over time after inoculation. The maximum bacterial density in coculture was not significantly different from the maximum bacterial density in monoculture with or without sucrose by two-tailed Student's t-tests (p > 0.05).

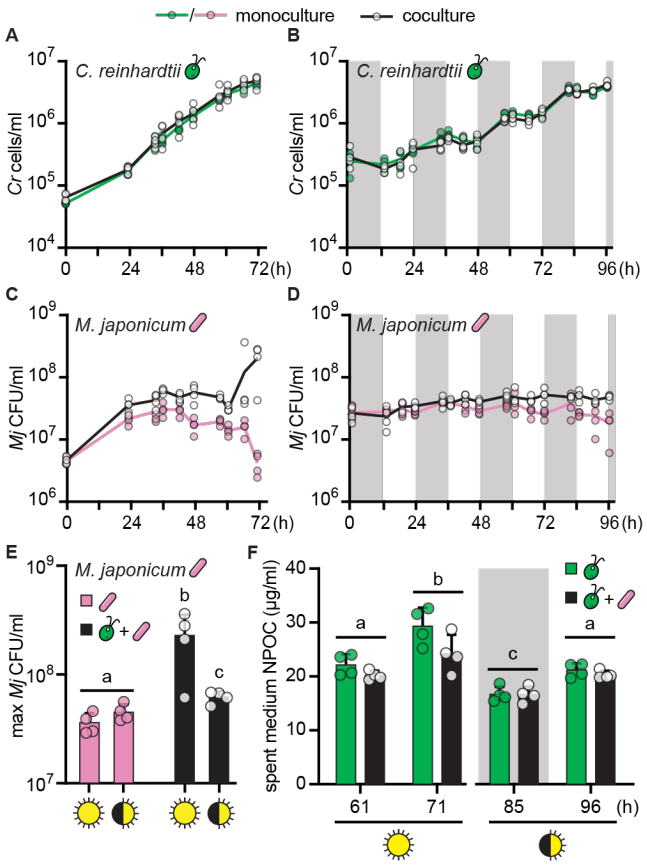

Figure 2: Coculture light regime impacts organic carbon release and *M. japonicum* growth. Quadruplicate (n = 4) monocultures (colors) and cocultures (black and white) were bubbled with air and shaken at 125 rpm. Cultures were inoculated to reach the same final algal cell density at the end of the experiment. (A, B) Growth of cell wall reduced strain CC-5390 in continuous light or diurnal light (12-h-light/12-h-dark), respectively, with and without *M. japonicum*. The grey backgrounds indicate sample timepoints that occurred during the dark phase. Under diurnal light, CC-5390 exhibits synchronous growth, doubling roughly once per day upon nightfall. (C, D) *M. japonicum* growth under the continuous and diurnal light regimes, respectively, with and without CC-5390. (E) Maximum bacterial density achieved under the various trophic conditions tested. (F) NPOC in spent medium from CC-5390 and cocultures sampled at the indicated times from the continuous and diurnal light regimes in (A) and (B), respectively. Lower-case letters indicate

significantly different groups by paired two-tailed Student's *t*-test ($p < 0.05$). Error bars represent the standard deviation from the mean.

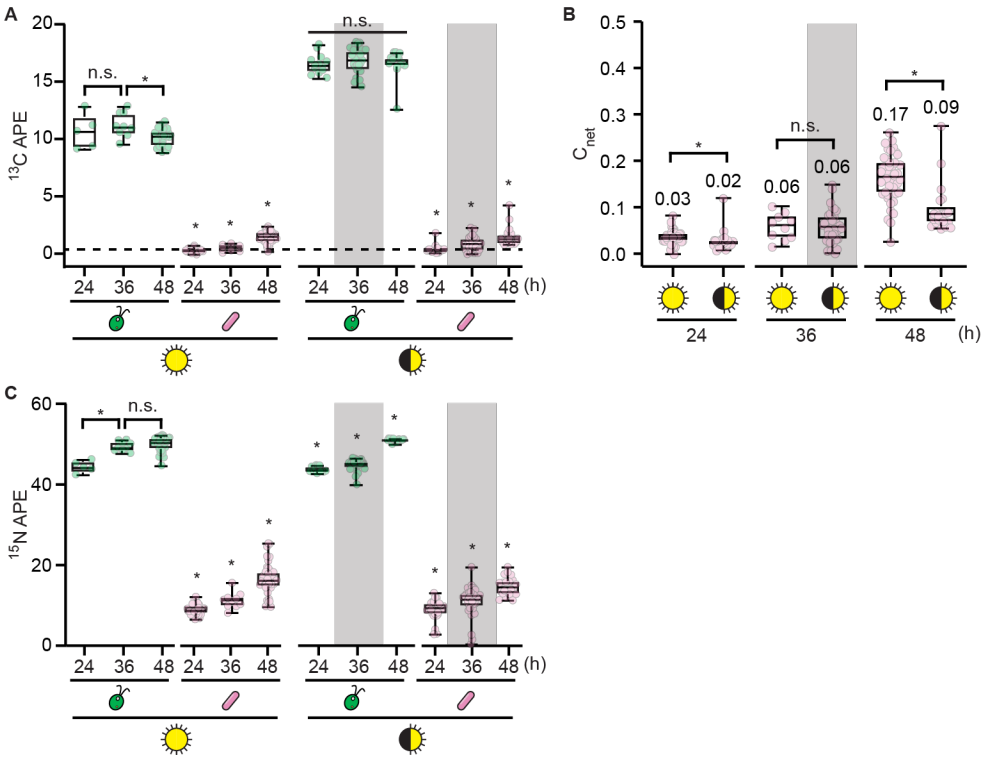

Figure 3: Stable isotope probing demonstrates carbon flux in continuous and diurnal light. Duplicate cocultures (n = 2) of CC-5390 and *M. japonicum* were grown as described in Fig. 2 but with 50% of their NH_4^+ provided as ^{15}N and with $^{13}CO_2$ added to the air starting 13 h after inoculation. Isotope enrichment was measured using nanoSIMS at the indicated times after inoculation. The grey backgrounds indicate sample timepoints that occurred during the dark phase. (A) ^{13}C atom percent enrichment (APE) data of $n \geq 5$ individual cells grown under continuous light or diurnal light. The dashed lines represent the maximum ^{13}C APE that occurred in *M. japonicum* monoculture controls provided sucrose as a result of nonspecific background or direct CO_2 incorporation during heterotrophic growth; see SI Fig. 6 for more details. Asterisks indicate significant differences over time in a given culture by two-tailed Student's t-test ($p <$ 0.05). (B) C_{net} of *M. japonicum* cells ($n \geq 10$), calculated relative to the algal biomass as the source. Median values are indicated, and asterisks indicate significant differences by two-tailed Student's t-test ($p < 0.05$). (C) ^{15}N APE data of $n \geq 5$ individual cells grown under continuous

light or diurnal light. Asterisks indicate significant differences over time in a given culture by two-tailed Student's *t*-test ($p < 0.05$).

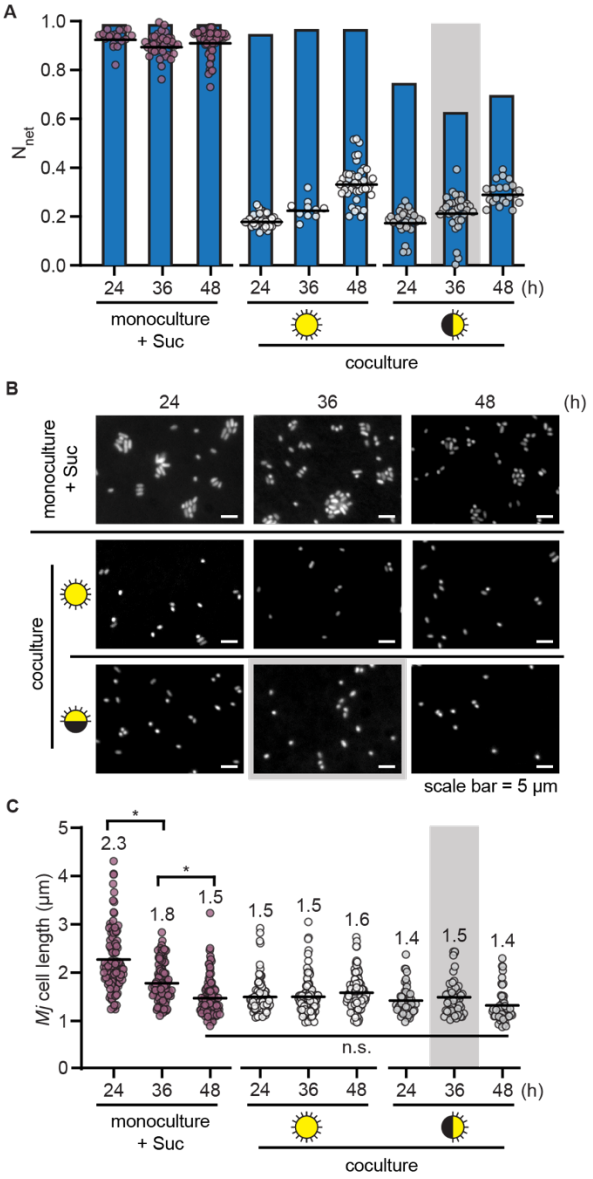

Figure 4: *M. japonicum* undergoes reductive division upon depletion of sucrose and during algal coculture. Duplicate cultures (n = 2) (monoculture with 150 µg/ml sucrose or coculture under continuous light or diurnal light) were grown as described in Fig. 2 but with 50% of their NH_4^+ provided as ^{15}N and with $^{13}CO_2$ added to the air starting 13 h after inoculation. Isotope enrichment was measured using nanoSIMS and cells were imaged by fluorescence microscopy at the indicated times after inoculation. The grey backgrounds indicate sample timepoints that occurred during the dark phase. (A) N_{net} of *M. japonicum* cells ($n \geq 10$) (circles) relative to the

calculated expected N_{net} (blue bars) if each doubling in CFU/ml represented a doubling in biomass (SI Fig. 8). Black lines represent mean values. (B) Representative fluorescence microscopy images of cells stained with DAPI. (C) Cell length of $n \geq 50$ *M. japonicum* cells per culture type ($n \geq 25$ cells from each of the duplicate cultures) measured using ImageJ. Mean cell length is indicated, and asterisks indicate significant differences by two-tailed Student's *t*-test ($p < 0.05$).

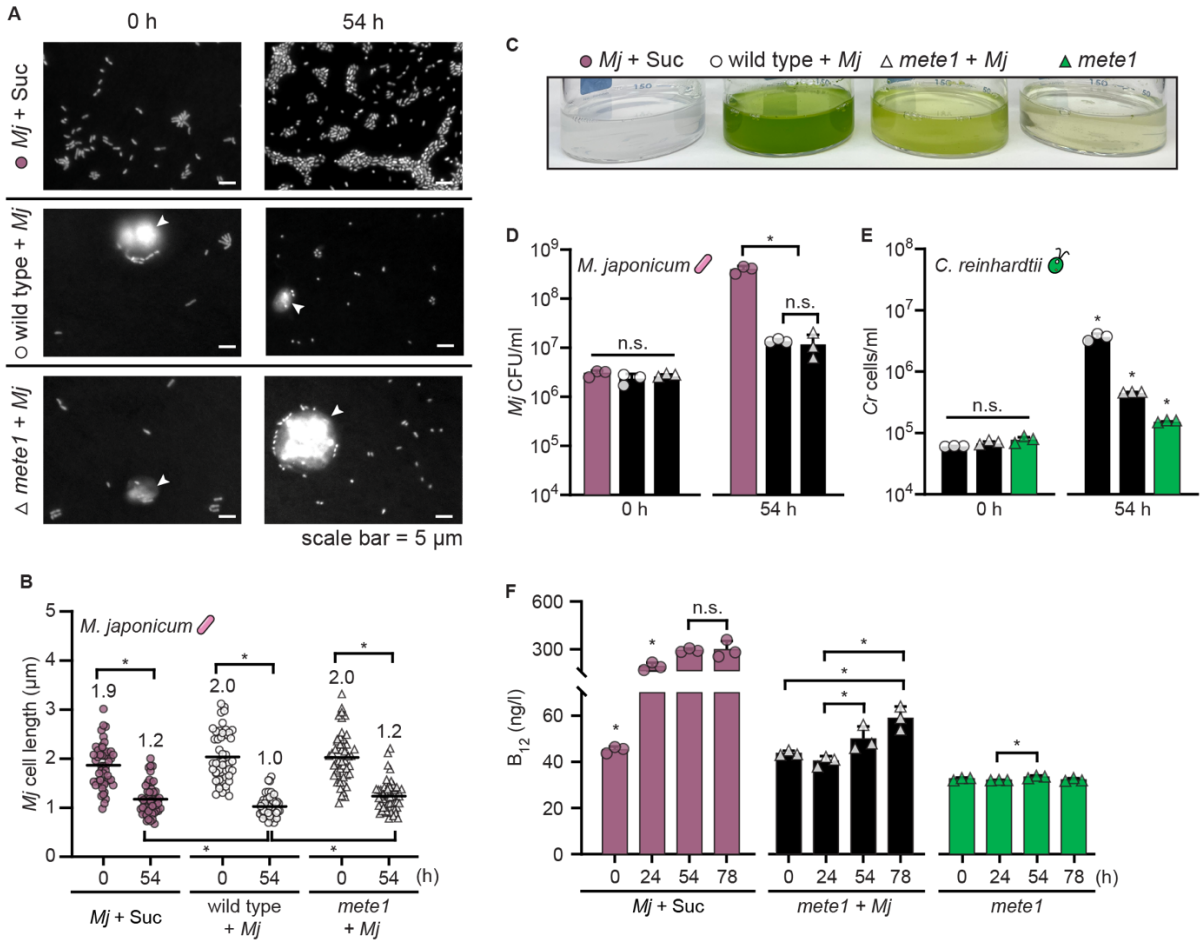

Figure 5: *M. japonicum* delivers vitamin B_{12} to *C. reinhardtii* despite reductive division. Triplicate cultures (n = 3) were maintained under continuous light, shaken at 130 rpm, and assayed at the indicated times after inoculation. (A) Representative fluorescence microscopy images of *M. japonicum* with 150 µg/ml sucrose, in coculture with *C. reinhardtii* wild type, and in coculture with *C. reinhardtii mete1*. Cells were stained with DAPI, and *C. reinhardtii* cells are indicated with white arrowheads. (B) Length of *M. japonicum* cells (n = 50, 10–20 cells from each of the three triplicate cultures) measured using ImageJ. Mean cell length is indicated. (C) Representative image of cultures 54 h after inoculation. (D) *M. japonicum* density in monoculture with 150 µg/ml sucrose (pink bars) or in coculture (black bars) with wild-type (circles) and *mete1 C. reinhardtii* (triangles), estimated as CFU/ml. (E) Cell density of *C.*

reinhardtii wild type (circles) or *mete1* (triangles) in coculture (black bars) and of *mete1* alone without added vitamin B_{12} (green bars). (F) Concentration of vitamin B_{12} in cultures measured using an *E. coli* bioassay. Error bars represent the standard deviation from the mean, and asterisks indicate significant differences by two-tailed Student's *t*-test ($p < 0.05$).

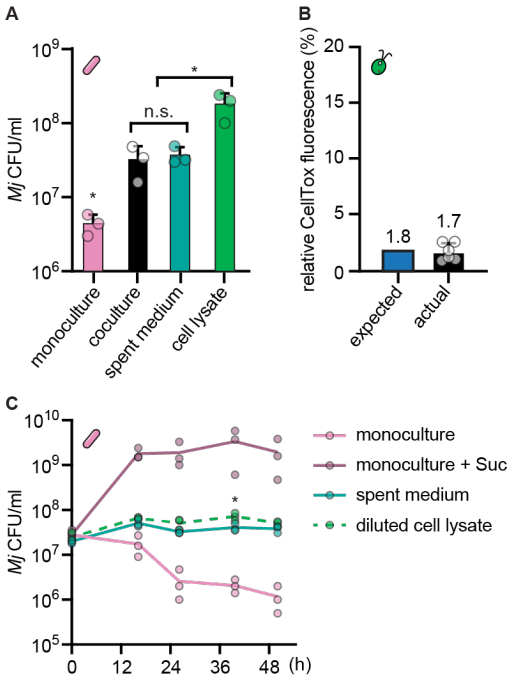

Figure 6: A small degree of algal lysis can explain the *M. japonicum* growth that occurs in coculture. Triplicate cultures (n = 3) of wild-type *C. reinhardtii* were grown under continuous light and shaken at 125 rpm for 24 h, reaching 1–4x10^6 cells/ml. These cultures were then split and used to generate parallel live algal cultures, algal spent media, and algal cell lysate, each then inoculated with *M. japonicum* in triplicate (n = 3). (A) *M. japonicum* density 45 h after inoculation in monoculture with no reduced carbon source, coculture with live *C. reinhardtii* cells, *C. reinhardtii* spent medium, or *C. reinhardtii* cell lysate. Asterisks indicate significant differences by two-tailed Student's t-test ($p < 0.05$). (B) The approximate degree of *C. reinhardtii* cell lysis required to explain *M. japonicum* growth in coculture based on *M. japonicum* growth yield in *C. reinhardtii* cell lysate (blue bar), and the degree of *C. reinhardtii* cell lysis measured in the cultures used for the experiment in panel (A) by CellTox Green fluorescence, reported relative to a 100% killed control. The expected value and the mean value are indicated. (C) *M. japonicum* density in triplicate cultures (n = 3) over time after inoculation in monoculture with or without 150 µg/ml sucrose, in *C. reinhardtii* spent medium, or in *C.*

reinhardtii cell lysate when diluted to the same NPOC concentration as the spent medium. The asterisk indicates a significant difference in density between spent medium and diluted cell lysate 40 h after inoculation by Student's *t*-test ($p < 0.05$); density was not significantly different between these two conditions at the other timepoints examined ($p > 0.05$). Error bars represent the standard deviation from the mean.